Supporting Information

Resonant Metagratings for Spectral and Angular Control of Light for Colored Rooftop Photovoltaics

Floris Uleman,[1,2] Verena Neder*,[1,2] Andrea Cordaro,[1,2] Andrea Alù,[3] and Albert Polman[2]

[1]Institute of Physics, University of Amsterdam

Science Park 904, 1098 XH Amsterdam, the Netherlands

[2]Center for Nanophotonics, NWO-Institute AMOLF

Science Park 104, 1098 XG, Amsterdam, the Netherlands

[3]Photonics Initiative, Advanced Science Research Center, City University of New York,

New York, NY 10031, USA

*v.neder@amolf.nl

1. Scattering of Mie resonator

Figure S1 shows the simulated[1,2] normalized scattering cross section (optical scattering cross section normalized by the geometrical cross section) for a Si NW of height h=175 nm and width w=110 nm on a sapphire substrate, illuminated at normal incidence by a plane wave polarized perpendicularly to the axes of the NW (TE polarization). The peak around λ=720 nm marks the excitation of the magnetic dipole mode (MD), while higher order modes appear at shorter wavelengths. The inset of Figure S1 shows the H field intensity profile at the MD resonance. The resonant wavelength of such modes can be easily tuned by changing the size of the scatterer, thus enabling the required spectral control. Comparing the scattering cross section with the spectrum of reflectance in Figure 1 b in the main text, raises the question why the reflectance peak is located at λ=650 nm for the scatterer in a periodic metagrating. The angular radiation pattern of the modes of the single scatterer determines the scattering towards different directions. However, light can only be scattered to the accessible channels (reflection, transmission, diffraction). The spectrum to those fixed pathways is thus given by the frequency dependence of the radiation pattern. But there are other effects that have to be taken into account. In the case of this work, the reflection from the substrate cancels the 0^{th} order reflection pathway and the light is thus funneled to the diffraction orders or to transmission, even though the radiation pattern might as well radiate upwards. Also, if the scatterers are getting closer there might be coupling between the particles and new modes appear that can influence the radiation direction. The exact analysis of the modes and their radiation patterns and interaction is beyond the scope of this work. To this end, a particle with resonances in the wavelength range of interest

(λ = 630 nm – 670 nm) was taken as a starting point and optimized as unit cell in a metagrating to achieve high diffraction to the 1st order and as such cancellation of the 0th order.

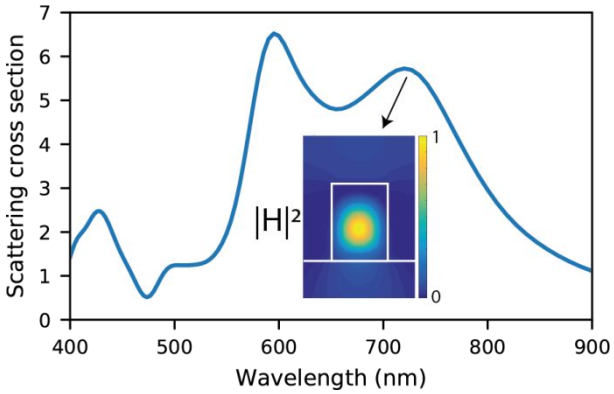

Figure S1 Simulated normalized scattering cross section of a single silicon nanowire (w=110 nm, h=175 nm) on top of a sapphire substrate. The inset shows the magnetic field intensity profile at the magnetic dipole resonance at 720 nm.

2. Metagrating efficiency

As highlighted in the main text, our metagrating design efficiently steers light into the 1st diffraction order by canceling the specular reflection (0th order). This is due to the destructive interference between light directly reflected off the substrate and light that is resonantly scattered by the nanowires. In Figure S2, this effect is illustrated by plotting the simulated reflectance of a metagrating while varying the index of the substrate from *n*=1 to *n*=2. This in turn modifies the relative contribution between the scattered light and the light reflected non-resonantly from the sapphire substrate. The latter contribution is zero when n=1.

The simulated metagrating is the same as in Fig. 1b in the main text (width = 110 nm, height = 175 nm, pitch = 900 nm). As the substrate's index is increased, the relative specular reflectance to the 0th order shows a decrease (Fig. S2 a) while the diffraction to the 1st order increases (Fig. S2 b) for an illumination wavelength close to the resonance (λ= 650 nm).

In fact, without the substrate the nanowires scatter isotropically, while introducing a substrate and increasing its index, the specular reflection is suppressed and the diffraction efficiency increases. To corroborate this, we plot the extreme cases of a low and a high substrate index in Fig. S2c. With no substrate in place (Fig. S2 c – lower panel), the reflectance to the 0th order is equal to the scattering towards the 1st order (isotropic scattering). On the other hand, for a substrate with index n=2 (Fig. S2 c – upper panel), the 0th order reflectance is completely suppressed. In the case of our experiment the substrate is sapphire (index = 1.7) and the 0th order reflection can almost be canceled completely.

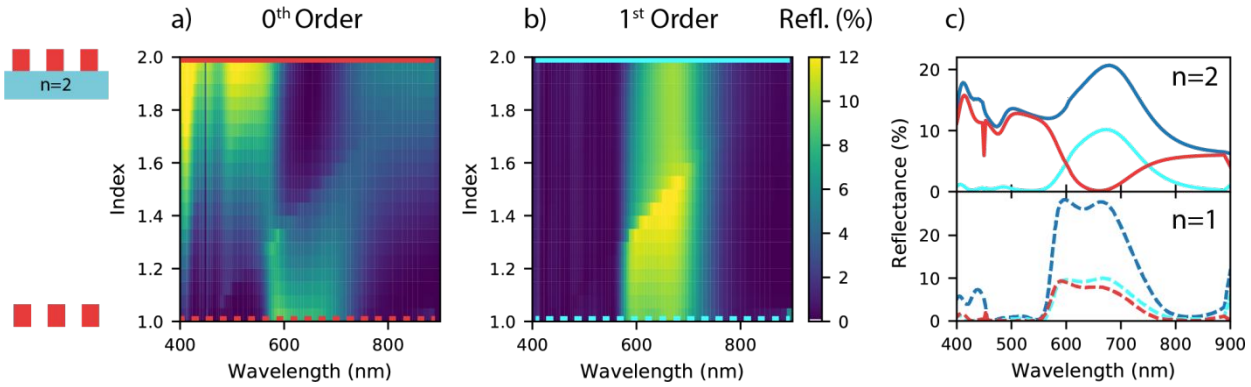

Figure S2 Simulated reflectance of a metagrating of silicon resonators (*w*=110 nm, *h*=175 nm, *p*=900 nm) with changing substrate index (n=1-2). Front inset: Schematic of metagrating on a substrate or without substrate. **a)** Specular reflectance (0th order) and **b)** diffraction into 1st order. The cyan and red lines indicate the crosscuts of specular reflectance and diffraction plotted in c) respectively. Reflectance above 12% is saturated for better visibility. **c)** Bottom: The total reflectance (blue line), specular reflectance (cyan line) and diffraction into the first order (red line) of a metagrating without a substrate (n=1); Top: Same as bottom graph, with metagrating on substrate with index n=2.

3. Parameter overview

The specific parameters of the metagratings composing the supercell are summarized in Table S1.

Table S1. Overview of design parameters and efficiencies of all metagratings

pitch [nm]	width [nm]	number of particles	angle	Reflectance at λ = 650 nm (%)	Diffraction efficiency to 1st order (%)
675	120	6	74	26.4	90.5
700	120	7	68	29.0	92.6
725	120	7	64	30.0	93.4
750	120	7	60	26.1	95.9
775	120	7	57	24.9	96.7

800	120	7	54	23.7	97.1
825	120	8	52	22.6	97.3
850	120	8	50	21.4	97.4
875	120	8	48	20.2	97.3
900	120	9	46	18.9	97.0
925	120	9	45	17.6	96.6
925*	120	9	45	17.6	96.9
950	120	9	43	16.4	96.1
975	120	9	42	15.2	95.3
1000	110	10	41	14.9	99.2
1025	110	9	39	13.6	98.6
1050	110	10	38	12.5	97.6
1075	110	10	37	11.4	96.2
1100	110	10	36	10.0	93.3

1125	110	10	35	9.0	90.8
1150	100	10	34	9.4	90.9
1200	100	11	33	8.0	83.4
1225	100	11	32	7.5	78.7
1250	100	11	31	7.2	73.5
1300	100	12	30	10.1	55.3

*The metagrating with a pitch of 925 nm was accidently put twice in the design/fabrication.

4. Reflectance with changing pitch

The metasurface is composed of metagratings with changing pitch in order to create a large range of diffraction angles as explained in the main text. Every individual metagrating was optimized to maximize the diffraction towards the 1^{st} orders in a bandwidth of λ= 630 nm – 670 nm. Figure S3 shows the simulated reflectance spectrum to 1^{st} and 0^{th} orders as the metagrating pitch is increased (p=700 nm – 1300 nm) while the unit cell is kept constant (NWs size w=110 nm, h=175 nm).

The strength of the reflectance is related to the strength of the scattering of the unit cell. Consequently, with increasing distance between the scatterers, the overall reflectance is decreasing and so is the diffraction. For the supercell design, the peak of reflectance lies at 680 nm, which stems from the combined diffraction spectra of the different metagratings (See Figure 3 of main text). Observing the 0^{th} order reflectance, it is easy to notice that the minimum does not change much between the different pitches. This is due to the fact that the cancellation process is mainly driven by the interference with reflectance of the substrate and does not change much between different pitches.

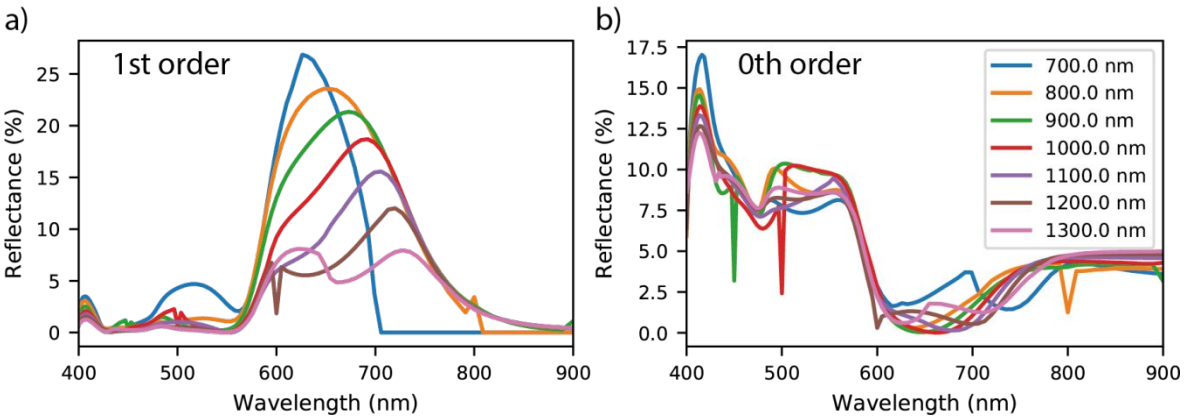

Figure S3 Simulated reflectance of metagratings of silicon resonators on a sapphire substrate (w=110 nm, h=175 nm, p=700 nm – 1300 nm) into 1st order and 0th order

5. Analysis of angle of incidence

The metasurface was optimized for normally incident light. As the position of the sun is changing during the day, it is important to study the operation of the metasurface as the angle of incidence is changed. In Figure S4 a, the simulated angular reflectance of the full metasurface is shown with angles of incidence between 10 – 45°. At λ = 650 nm the angular scattering still follows the desired cosine distribution (grey dashed line), however, with the shifts in angles given by the grating equation. At large angle of incidence, the metasurface supports as well 2nd order diffraction at λ = 650 nm that contribute to a wide range of reflected angles.

Next, the reflectance spectra of a metagrating with a pitch of p = 900 nm is shown in Figure S4b as the angle of incidence is swept the same range (10-45°). For small angles (around 10°) the resonant reflectance of the design is pretty stable. For larger incoming angles (20°) the resonant backward scattering seems to disappear, but the cancellation process of the specular reflection is still efficient. For even larger angles (30° and 45°), the reflectance peaks again around λ = 700 nm, and specular reflection is still cancelled. As mentioned earlier, the precise change of modes is out of the scope of this study. However, the arguments for the cancellation process still hold for different angles of incidence.

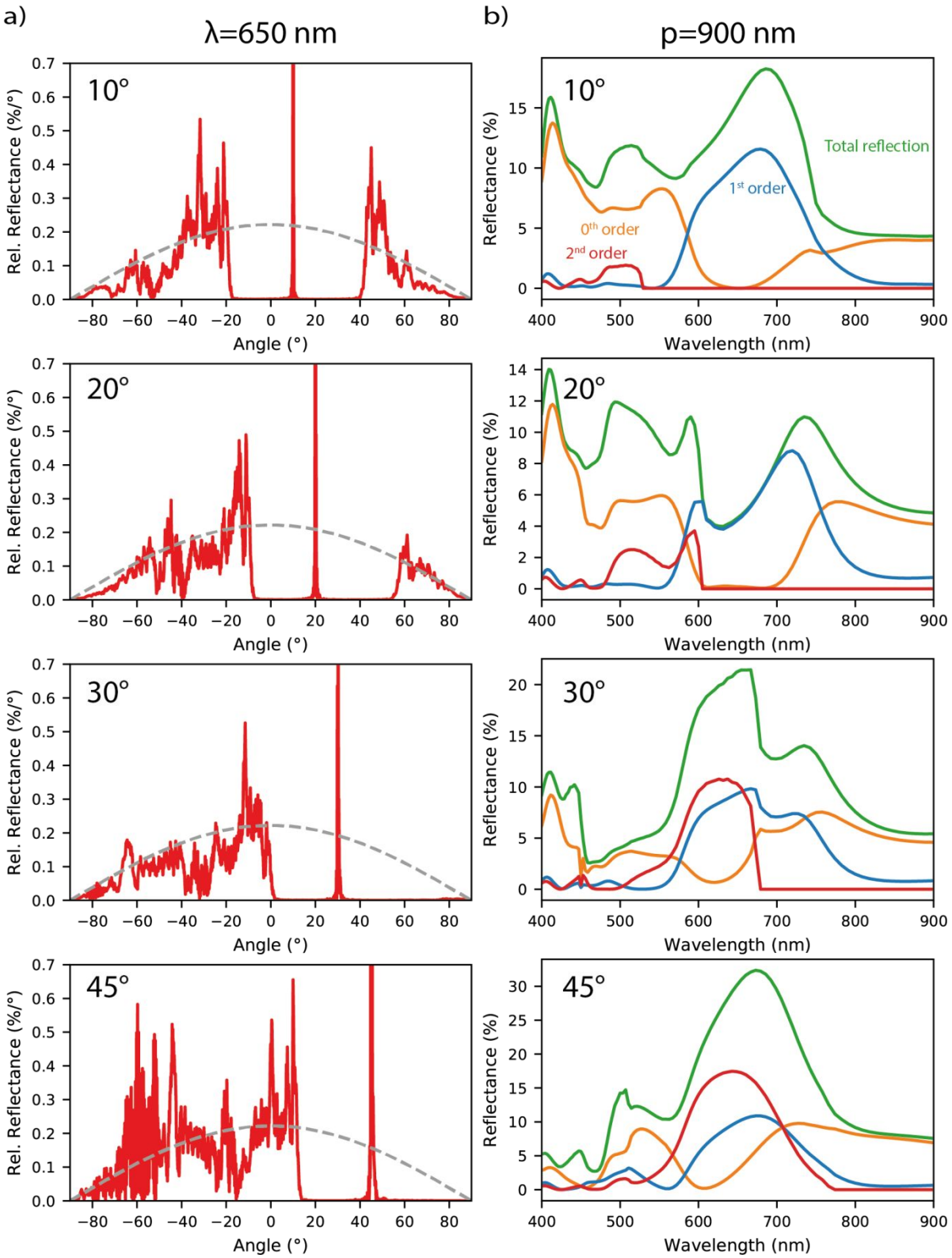

Figure S4 Analysis of changing angle of incidence a) Simulated angular reflectance at λ = 650 nm of full metasurface for angles from 10° - 45°. b) Simulated reflectance of metagrating as in Figure 1 c) with changing angle of incidence from 10° - 45°. The total reflectance (green line) is composed of specular reflectance (orange line), 1st order diffraction (blue line) and 2nd order diffraction (red line).

6. Integrating sphere measurement setup

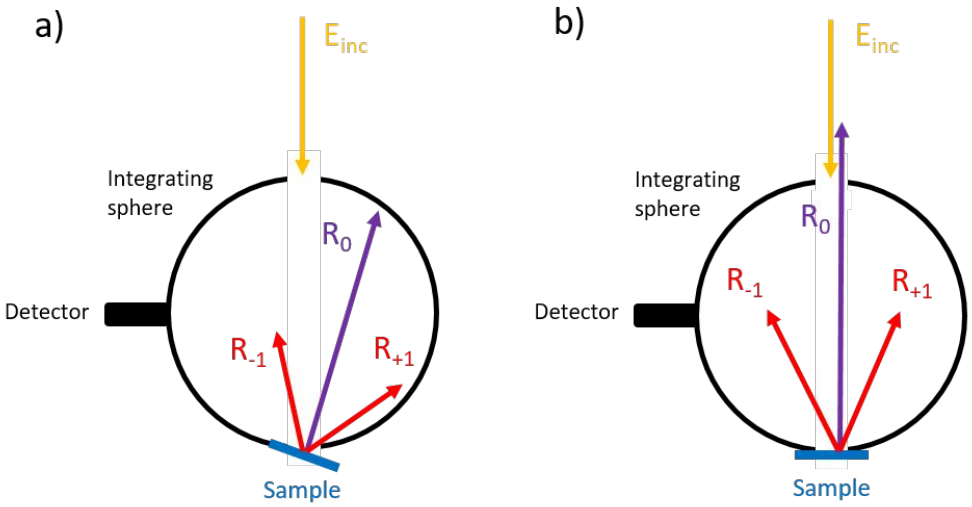

Figure S5 Integrating sphere setup a) Configuration with tilted sample; all scattered light is collected. b) Configuration with sample perpendicular to incoming light; specular reflection is not collected.

We measured the scattering of the sample using an integrating sphere. There are two methods of measurements; either to measure the total reflection (Figure S5 a; specular reflection plus all diffraction orders) or only the diffraction (Figure S5 b; no specular reflection). For the first method, the conventional setup of the integrating sphere is used. The sample is tilted at the back of the sphere, such that all reflection is collected by the detector. In the second method the sample is placed perpendicular to the incoming light at the back of the integrating sphere. In the latter case, the specular reflected beam can escape from the front opening of the sphere, and only scattered and diffracted light is collected by the spectrometer. The specular reflectance shown in Figure 3a of the main text is determined by the subtraction of two measurements by the two different methods; the diffraction measurement is subtracted from the total reflectance. For the scattered spectrum in that same Figure the second method of the setup was used.

(1) Lumerical Inc. https://www.lumerical.com/products/.

(2) Palik, E. D. *Handbook of Optical Constants of Solids*; Academic: New York, 1985.